An experimental study of diabatic spiral vortex flow

C. C. Wan* and J. E. R. Coney*

In spiral vortex flow, between concentric cylinders with the inner cylinder rotating and the outer stationary, the addition of a thermal gradient across the gap is a known complicating factor. The present diabatic study for narrow and wide gaps (radius ratios $N = 0.955$ and $N = 0.8$), with a heated outer and adiabatic inner cylinder, was undertaken to investigate this problem. The heat transfer characteristics and the modes of transition have been investigated together with the relationship between them. Using standard on-line digital computer techniques, the onset of vortex flow and its higher transitions have been shown to cause a sharp increase in Nusselt number. At higher Taylor numbers, of the order of 10^6, a marked change in the Nusselt number occurs with the onset of the transition to periodic turbulent vortex flow. Outer wall heating is seen to affect the modes of transition. Diabatic critical Taylor numbers are much higher than those for adiabatic conditions and are found to depend on the close approach of the vortices to the outer wall

Key words: *heat transfer, turbulent flow, vortices, flow transitions*

Viscous fluid flow through a concentric annular gap occurs in many engineering applications. Where the inner cylinder rotates and the outer is stationary, at a sufficiently high inner cylinder speed, the ratio of the centrifugal and viscous forces reaches a critical value at which the flow pattern assumes the form of contra-rotating toroidal vortices termed Taylor vortices. In engineering practice, the formation of these vortices aids drying and extraction processes in the chemical industry. In clinical blood oxygenators, Taylor vortex flow is being investigated as a means of enhancing flow mixing and mass diffusion to prevent haemolysis[1]. In the exploration of off-shore oil and gas fields, similar flows occur in drilling mud between the rotating drill and the stationary outer casing.

The attention given to the problem of air cooling in electric motors has resulted in a number of important contributions to this field[2–4], the main objective of these investigations being to provide substantial experimental data, as well as theoretical predictions for the designer of such electrical machines; the most common configuration studied was that of a heated inner rotating cylinder with or without an imposed axial flow. The analogy solutions obtained from friction or torque measurements provided a good comparison with the heat transfer data and agreement was generally close.

A thermal gradient across an annular gap gives variations in density and viscosity, hence affecting free convection. With the inner cylinder rotating, these effects will interact with the centrifugal force field, caused by the rotation, to bring about an earlier or later onset of vortex instability compared with the adiabatic condition. According to Rayleigh's criterion, when the circulation increases radially outwards, the flow is stable, neglecting the effects of a density gradient. Assuming such a gradient, Fung and Kurzweg[5] analysed the stability of inviscid swirling flows. They found that such a flow is stable if the density is a monotonically increasing function of radius, provided the radial variations in both angular and axial velocity components are small. The confirmation of these results was provided by Withjack and Chen[6] for Taylor vortex flow, using stratified salt solutions and a wide gap configuration with an annular radius ratio of $N = 0.2$. Walowit *et al*[7] and Becker and Kaye[8] concluded from their computations that the effect of heating the outer wall was to provide a further destabilisation to the flow. Viscosity in a fluid is also known to provide a stabilising effect. The variation of the viscosity of air with temperature, however, is small and hence the stabilising effect of a temperature gradient, in this respect, is not great.

It must be noted that all the theoretical approaches mentioned so far have neglected the effects of gravity in their assumptions. Snyder and Karlsson[9] experimented with a vertical apparatus and discovered that the effects of gravity were sufficient to promote free convection in the annulus. The resulting convective flow was described as having a cubic profile, symmetrical about the centre of the gap. The detection of subcritical wavy disturbances due to axial convection was a unique feature of their experiments.

With an imposed axial flow, however, the addition of the velocity profile is a further complication. Snyder[10] and Karlsson and Snyder[11] suggested that, in the presence of a low axial Reynolds number, the stability of flow depends greatly on the combined parabolic and cubic velocity profiles but at higher

* Department of Mechanical Engineering, University of Leeds, Leeds, UK, LS2 9JT
Received 18 July 1981 and accepted for publication on 2 September 1981

axial Reynolds numbers the convective motion becomes less marked and a strong coupling exists between the imposed axial flow and the rotational flow. It was found that the position of the 'inflection point' of the parabolic profile was crucial in determining stability and that the dependence of the stability curve on the imposed axial flow commences when this point on the profile is displaced. Snyder[10] found that at higher flows, the measured values of the Taylor number for vortex flow in diabatic and adiabatic conditions tended to coincide. The recent work of Sorour and Coney[12] indicated that at low axial Reynolds numbers, cell length and drift velocity were significantly affected in that the wavelength was compressed and the drift velocity increased compared with the case of zero axial flow.

Summarising, there have been extensive analytical and experimental investigations into the hydrodynamics and heat transfer characteristics for zero axial flow but little work has been done so far for the condition of an imposed axial flow. This paper presents a study of the heat transfer characteristics and the transition modes of diabatic spiral vortex flow, where the outer wall is heated and the rotating inner wall is adiabatic. The digital techniques developed by the authors[13] were applied to the study of the flow transitions, while relating them to the heat transfer results. It is envisaged that improved knowledge of the hydrodynamics and heat transfer characteristics of spiral vortex flow will lead eventually to improved designs of rotating machinery, as well as providing an understanding of the evolution of turbulence in such confined flows.

Apparatus

A detailed description of the apparatus is given by Simmers and Coney[14]. The working fluid, air, was passed down a vertical concentric annular gap 1820 mm long, the mass flow rate of air being measured by orifice plates calibrated according to BS 1042. Outer wall heating was provided by a steam jacket placed around the outer stationary steel cylinder of inner diameter 139.7 mm. The inner rotating cylinder was of Tufnol, which served as an adiabatic surface. Two inner cylinders were used having outer diameters of 133.4 mm and 111.8 mm, giving annular radius ratios of 0.955 and 0.8 respectively. Twenty-nine measuring stations were distributed over the working section, providing access for velocity and temperature probes. The speed of the inner cylinder was measured by a magnetic pick-up and the pulses monitored by a high frequency digital counter. An accuracy of ±2% was obtained for low speeds and at high speeds the accuracy was ±5%.

Outer wall and fluid temperature measurements were made by chromel-alumel thermocouple probes contained in Tufnol traversing sleeves, and were recorded by a Solartron data logger. Fluid velocity measurements were made using DISA 55P71 parallel-wire probe. To compensate for the strong, rapid temperature fluctuations in the flow, a temperature compensator (DISA 55M14) was used in conjunction with a DISA 55M01 main unit. An on-line computer permitted recording of the analogue signals from the DISA equipment via an analogue to digital converter (adc). In the present

Notation

A	Area of heat transfer surface between two axial stations ($2\pi R_2 L^*$)
adc	Analogue to digital converter
b	Annular gap width ($R_2 - R_1$)
c_p	Specific heat of fluid at constant pressure
d_e	Equivalent diameter of annulus ($2b$)
f_N	Nyquist frequency
FFT	Fast Fourier transform
h_0	Overall convective heat transfer coefficient
i	Index for discrete time signal x_i
j	Index denoting a complex number
k	Index for data sequence
L^*	Distance between two axial stations
$\dot{m}$	Mass flow rate of fluid
M	Number of samples
N	Annular radius ratio (R_1/R_2)
Nu	Nusselt number ($h_0 d_e/\beta$)
Nu_β	Nusselt number for conduction
P_k	Power spectral density function
R	General radial co-ordinate
R'	Dimensionless gap position $(R-R_1)/(R_2-R_1)$
R_1	Radius of inner cylinder
R_2	Radius of outer cylinder
R_x	Autocorrelation function
$R_x(\tau)$	Autocorrelation function of signal $x(t)$
Re_a	Axial Reynolds number ($U_m d_e/\nu$)
Ta	Taylor number ($\Omega_1^2 R_1 b^3/\nu^2$ for a narrow gap) ($2\Omega_1^2 R_1^2 b^3/(R_1+R_2)\nu^2$ for a wide gap)
Ta^*	Taylor number ratio (Ta/Ta_c)
Ta_c	Critical Taylor number
u'	rms mean velocity fluctuation (sum of axial and rotational fluctuating velocity components)
$\bar{U}$	Mean effective velocity (vector sum of axial and tangential velocity components)
U_m	Mean axial velocity component
$x(t)$	Continuous time signal
x_i	Discrete representation of signal $x(t)$
X_k	Discrete Fourier integral
X_k^*	Complex conjugate of X_k
β	Thermal conductivity of fluid
Δt	Sample interval
$\Delta\theta_{LM}$	Logarithmic mean temperature difference
θ_1	Mean temperature of fluid at axial position 1
θ_2	Mean temperature of fluid at axial position 2
θ_w	Temperature of outer wall
μ	Dynamic viscosity of fluid
ν	Kinematic viscosity of fluid (μ/ρ)
ρ	Density of fluid
τ	Time delay of correlation function
Ω_1	Inner cylinder angular velocity

investigation, a VAX 11-780 32-bit computer was used to analyse the recorded signals in digital form, thus permitting spectrum analysis and autocorrelation of the hot wire signals. The general arrangements of the analogue and digital equipment have been described previously[13].

Procedure

Heat transfer and velocity measurements were made under the same conditions so as to be comparable. The overall heat transfer coefficient was calculated from:

$$h_0 \equiv \frac{\dot{m} c_p (\theta_1 - \theta_2)}{A \, \Delta\theta_{LM}} \tag{1}$$

where θ_1 and θ_2 are the average fluid temperatures at two axial stations. These stations were selected so that they were well within the fully developed region. Wall temperatures (θ_w) were recorded by five thermocouple probes placed flush with the outer wall between the two axial stations.

Having determined h_0, the Nusselt number, Nu, could be determined. Various axial flows were investigated for $500 \leq Re_a \leq 2800$ and for $Ta \leq 10^6$.

Digital recording techniques

Sampling of the hot wire signals by the adc was commenced when steady isothermal conditions had been achieved, the number of samples being 16384 with a sample interval, Δt, of 2 ms. To avoid the phenomenon of aliasing discussed by Otnes and Enochson[15], the Nyquist frequency (f_N) was chosen to be 500 Hz, since the hot-wire signals are well below this bandwidth. The correct choice of f_N is important so that spectral analyses of the signals, which do not give spurious harmonics occurring at higher frequencies or aliases, can be made. The problems of clipping, leakage and noise contamination, which are common in digital systems, were overcome or reduced so that the digital signal reconstructed on the computer bore a close resemblance to the analogue signal.

The data sequence was then partitioned into segments of 8192 samples for analysis. To obtain the power spectral estimates, data smoothing using a Hanning window was applied and the partitioned sequence transferred into the frequency domain by a fast Fourier transform (FFT) algorithm which computed:

$$X_k = \frac{1}{M} \sum_{i=1}^{M} x_i \exp\left(\frac{-j.2\pi ik}{M}\right) \tag{2}$$

The raw power spectral estimates were obtained from:

$$P_k = 2|X_k X_k^*| \tag{3}$$

The raw estimates were then divided by the energy of the smoothing function and linearly averaged over all the partitions to improve the accuracy and consistency of the estimates.

Calculation of the autocorrelation function was by the inverse FFT routine where the computation time is only a fraction of that required for the direct method. The resulting autocorrelation function $R_x(i)$ was given by:

$$R_x(i) = \frac{M}{M - i} \sum_{k=1}^{k=2M} P_k \exp\left(\frac{j\pi ik}{M}\right) \text{ for } k = 1, \ldots 2M \quad i = 1, \ldots \tau \tag{4}$$

The coefficient $R_x(\tau)$ was normalised with respect to $R_x(1)$ for comparison. Testing of the power spectrum and autocorrelation analysis was performed using deterministic signals, eg a sine or square wave. The resolution for a sample record of 8192 samples, using a Hanning window, was 0.01% of the Nyquist frequency.

The turbulence intensity ($u'/\bar{U}$) was also measured using two channels for the simultaneous recording of the voltage fluctuation and mean voltage respectively. Calibration of the flow on a DISA calibration unit permitted the linearisation of these voltages to give velocity values. The ratio $u'/\bar{U}$ was expressed as a percentage, each value being the average of six data records, each of 15 s duration per channel.

Heat transfer results

The heat transfer results for the narrow and wide gaps are shown in Figs 1 and 2 respectively as plots of Nusselt number against Taylor number. It can be seen that for low values of Ta, Nu is approximately constant, implying a primary laminar flow regime. The narrow gap only permits values of $Ta \leq 10^5$ and there is no evidence of any effects on heat transfer apart from the general increase of Nu with Re_a. The wide gap results, however, for various values of Re_a (Fig 2) provide a much greater variation in the heat transfer characteristics, owing to the wider range of Ta. In Fig 2, the effect of secondary vortex flow is

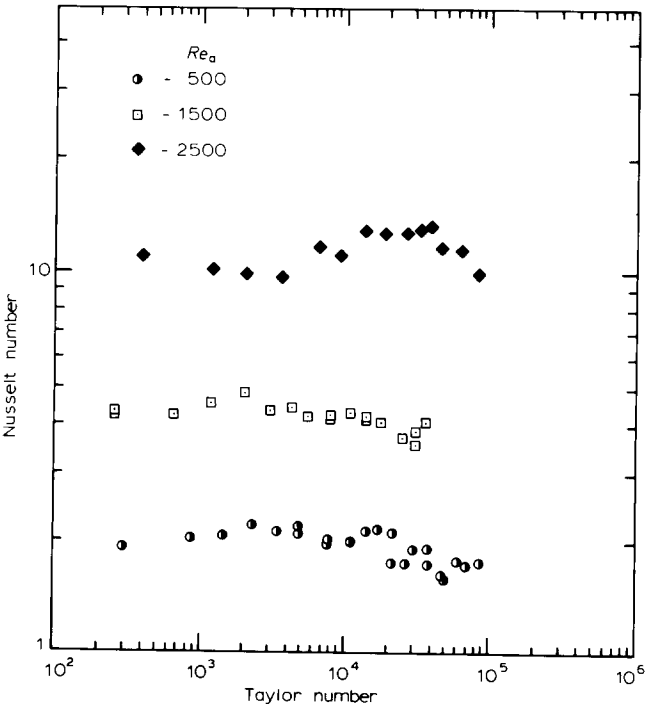

Fig 1 Variation of Nusselt number with Taylor number for N = 0.955

noticeable, being accompanied by a marked increase in Nu as Ta increases. In addition, increasing axial flows tend to delay the onset of this secondary flow regime. The decrease in Nu prior to this secondary regime seems to occur for the range of axial flows considered and cannot be explained at present.

Another feature of interest is the presence of a third flow regime, occurring at $Ta > 10^6$, which causes a change in the slope of the Nu versus Ta plot. This third regime is seen throughout the range $500 \leq Re_a \leq 2800$, with the slope increasing as Re_a increases. From the heat transfer point of view, this effect is undesirable, a decrease in the heat transfer rates occurring, especially for $Re_a \leq 1500$.

Transition modes

Narrow gap results (N = 0.955)

In Fig 3, spectrum and autocorrelation results for the diabatic flow transitions are presented for $Re_a = 500$ and $R' = 0.5$. Referring to Fig 3(b), the transition to vortex flow at $Ta = 19\,000$ is shown by a single spectral peak, f_1, with its associated harmonics; the second transition frequency peak, f_2, is just beginning to appear. Comparing this value of Ta_c with that for adiabatic conditions[13], the effect of a positive thermal gradient is seen not to be significant. At $Ta = 72\,700$ (Fig 3(e)) a chaotic spectrum denoting a weakly turbulent flow is observed where the peak f_2 disappears and f_1 still persists. Comparison with adiabatic spectral results indicates that the effect of a positive thermal gradient does not alter any of the

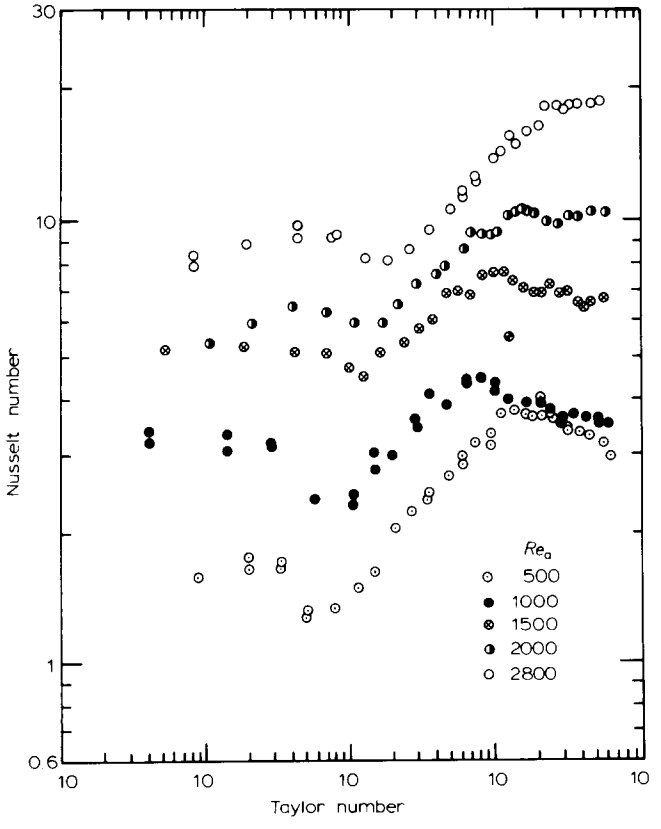

Fig 2 Variation of Nusselt number with Taylor number for N = *0.8*

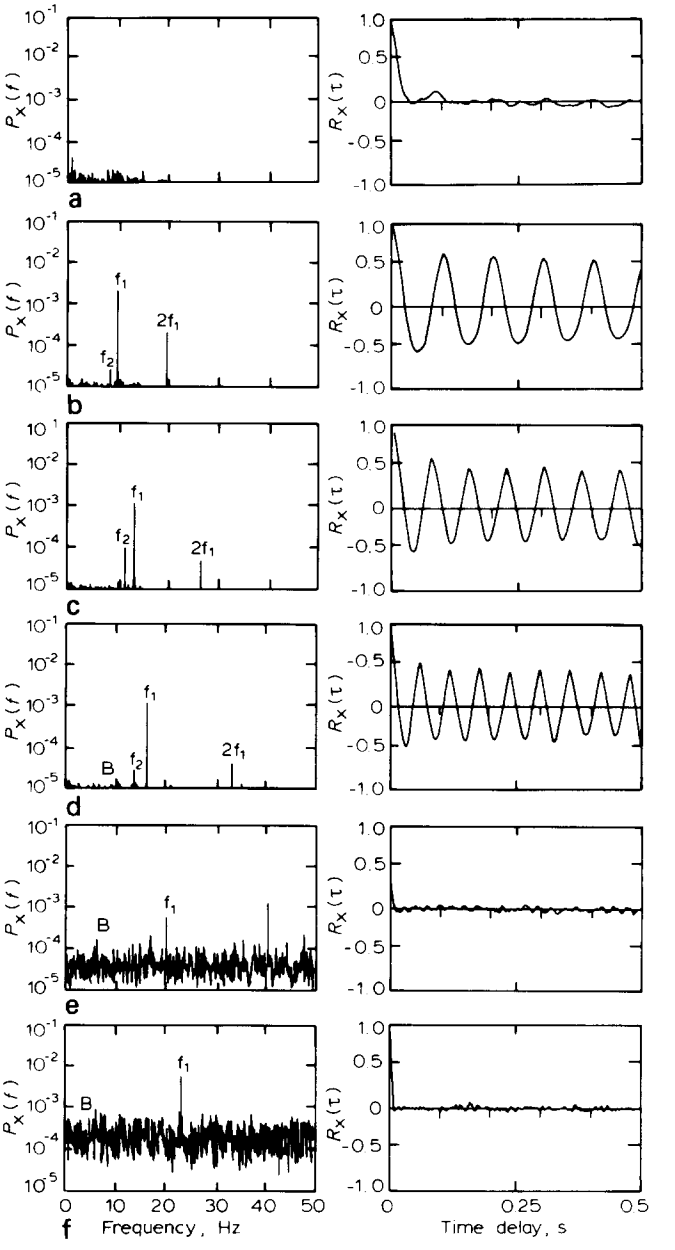

Fig 3 Diabatic power spectra (left) and auto-correlograms (right) for N = *0.955*, $Re_a = 500$, R' = *0.5. (a)* Ta = *0 (b)* Ta = *19 000 (c)* Ta = *31 800 (d)* Ta = *51 100 (e)* Ta = *72 700 (f)* Ta = *90 000*

spiral vortex transitions but tends to promote the general destabilisation of the higher transition modes in that they occur at lower values of Ta.

In Fig 3 the auto-correlograms correspond to the flow development, a periodic trace indicating vortex flow and its higher modes. As the spectral features broaden and become continuous, a loss in correlation results and the auto-correlograms become non-periodic.

Further investigations were made at $Re_a = 1500$ and 2500. Although the results are not presented here, they indicate that the effect of a higher axial flow tends to be destabilising, as was found for adiabatic flow. The spectra and auto-correlograms show the highly unstable nature of the flow transitions at these flows. Throughout the Ta range

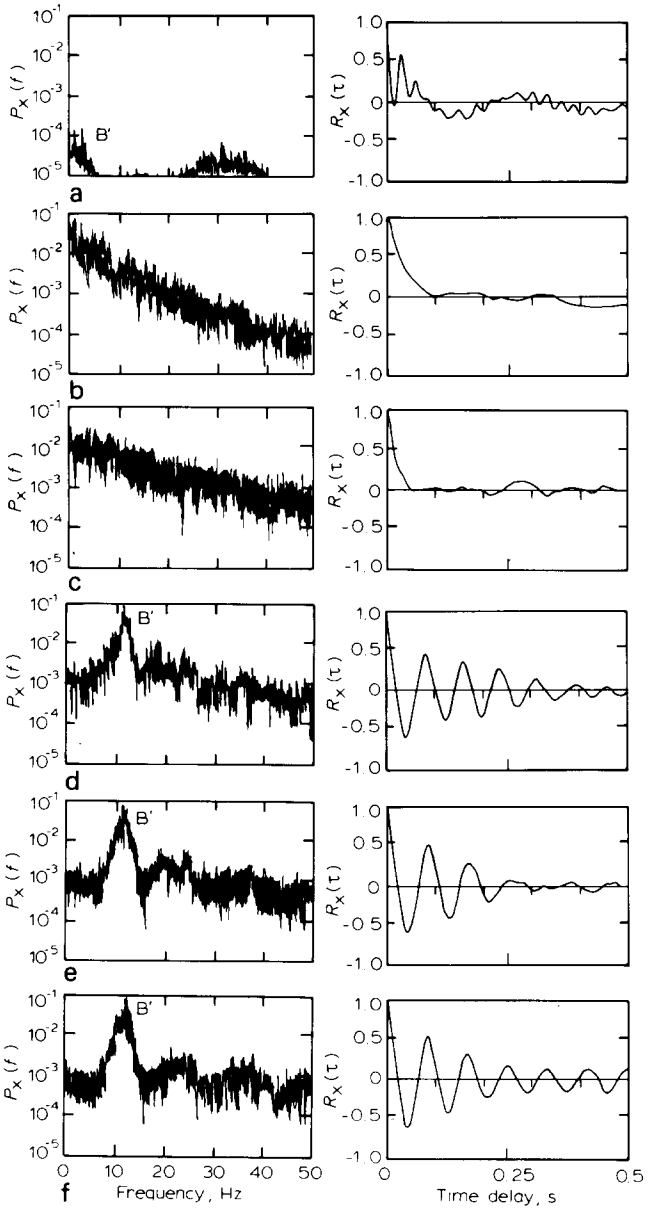

Fig 4 Diabatic power spectra (left) and autocorrelograms (right) for N = *0.8,* $Re_a = 500$ *and* R' = *0.75. (a)* Ta = *29 500 (b)* Ta = *86 800 (c)* Ta = 516×10^3 *(d)* Ta = 1.95×10^6 *(e)* Ta = 3.06×10^6 *(f)* Ta = 5.82×10^6

investigated, however, the spectral peak f_1 is clearly discernible and dominant.

Wide gap results (N = 0.8)

The diabatic spectral evolution and autocorrelograms for $Re_a = 500$ and $R' = 0.75$ are shown in Fig 4. It was expected that there would be greater variations of flow across the wide gap than across the narrow. Hence the probe position, $R' = 0.75$, was chosen because of the relevance of the results derived from it to the heat transfer occurring at the outer stationary surface of the annular gap. Compared with the narrow gap case, the spectra are very complicated and there are no sharply defined peaks. However, the transition from the periodic broadband peaks (B') to a chaotic mode and then to periodic flow again can be observed in both the spectra and autocorrelograms. These transitions are comparable to those obtained previously under adiabatic conditions[13].

The broadband peaks at $Ta = 29\,500$ (Fig 4(a)) suggest the presence of wavy vortices and, with increasing speeds, the spectra become more complex as further azimuthal waves are superimposed. The flow then apparently reorganises itself with a strong periodic motion around the annulus, suggesting the presence of turbulent vortices.

Results for $Re_a = 1500$ and 2500 (which are not presented here), show that the energy level of the complex spectra increases still further and the suppressing influence of the axial flow on the onset of the turbulent vortex transition is to be noted.

The flow transitions observed in the wide gap for $Re_a = 500$ can be related to the heat transfer results of Fig 2. It is evident that the onset of spiral vortex flow does not alter *Nu* markedly. The sharp increase in *Nu* may be associated with the chaotic spectra, denoting the increase in the wavy modes and possibly the general breakdown of the basic spiral vortex flow. In the light of this evidence, the close approach of the spiral vortex to the outer wall is followed by the increase in waviness and complexity of the vortex flow, thus causing a reduction of the thermal boundary layer and an enhancement of heat transfer. The third flow regime can be related to the turbulent vortex transition over the same *Ta* range. It appears that the energy transfer from the outer wall is impeded by the turbulent vortices, causing a change in the rates of heat transfer.

Turbulence intensity results

The turbulence intensity for both the wide and narrow gaps was investigated in order to provide further understanding of the diabatic spiral flow transitions. Fig 5 shows the narrow gap results for three axial

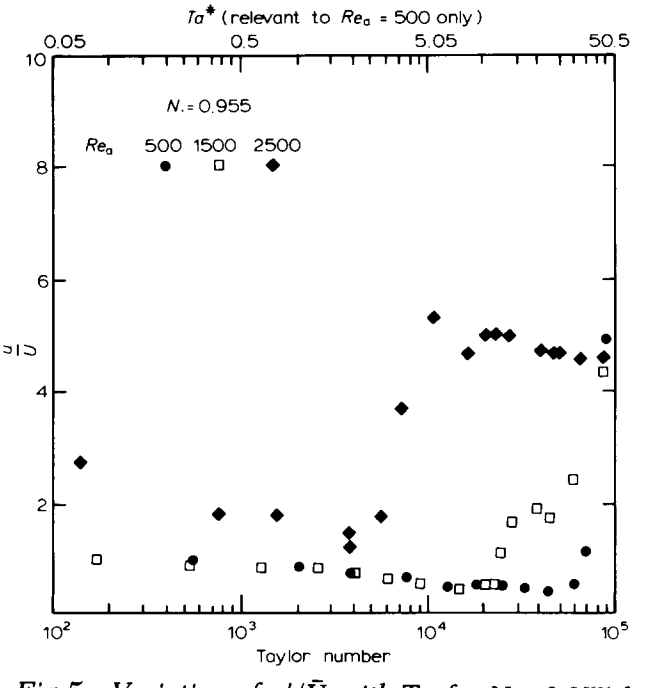

Fig 5 Variation of u'/Ū *with* Ta *for* N = *0.955 for the diabatic case*

flows at $R' = 0.50$. The turbulence intensity for $Re_a = 500$ is seen to increase sharply from a constant level with the onset of higher harmonics; the breakdown of the flow, with increasing axial flows, is accompanied by an earlier increase in $u'/\bar{U}$. At $Re_a = 2500$, high intensity values are obtained, confirming the high spectral energy levels observed in the associated spectra. Little difference is noted when comparing these with the adiabatic results[13] for $Re_a = 500$ since the spiral vortex transitions in diabatic and adiabatic conditions are very similar. However, the general destabilisation of the flow with increasing values of Re_a is clear.

The wide gap results are shown in Fig 6 for $R' = 0.75$. At $Re_a = 500$, the uniform intensity characteristic of spiral vortex flow increases sharply as the flow becomes more complex, resulting from the addition of azimuthal wavy modes. The transition to turbulent vortex flow at $Ta \approx 5 \times 10^5$ is marked by the trough in the graph for $Re_a = 500$. When this transition is complete, at $Ta > 2 \times 10^6$, a less intense motion ensues, leading to a decrease in the value of $u'/\bar{U}$; the spectra presented in Fig 4 confirm these observations.

The data for $Re_a = 1500$ show the damping influence of the high axial flow, the intensity $u'/\bar{U}$ remaining fairly constant after a sharp rise, for $Ta > 10^5$. The flow fluctuations become very strong at $Re_a = 2500$ and the damping influence of the axial flow is no longer evident, very little variation in $u'/\bar{U}$ being seen. It is noticeable that the sharp increases in $u'/\bar{U}$ for $Re_a = 500$ and 1500 are comparable to the heat transfer results in Fig 2 where the increase in Nu number occurs at similar Ta values.

Comparison with other investigations

The literature available in diabatic combined axial and rotational flow is scant. A recent investigation was carried out by Kuzay and Scott[16], but their results were limited to axial flows above those of the present

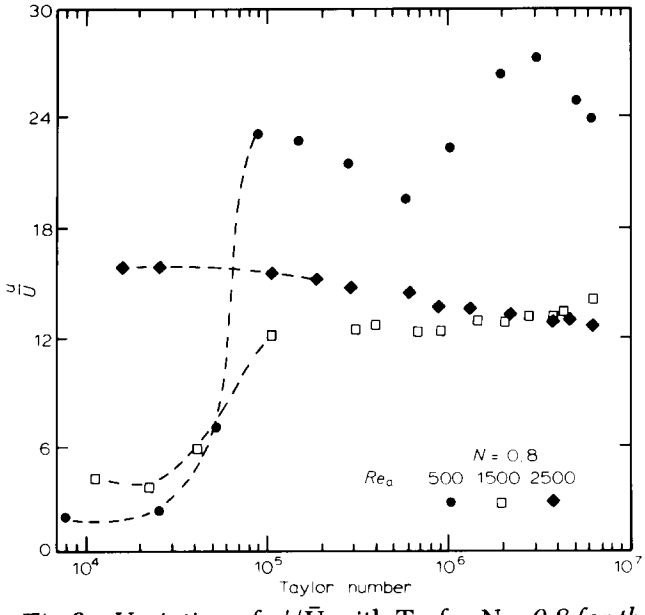

Fig 6 Variation of u'/Ū with Ta *for* N = *0.8 for the diabatic case*

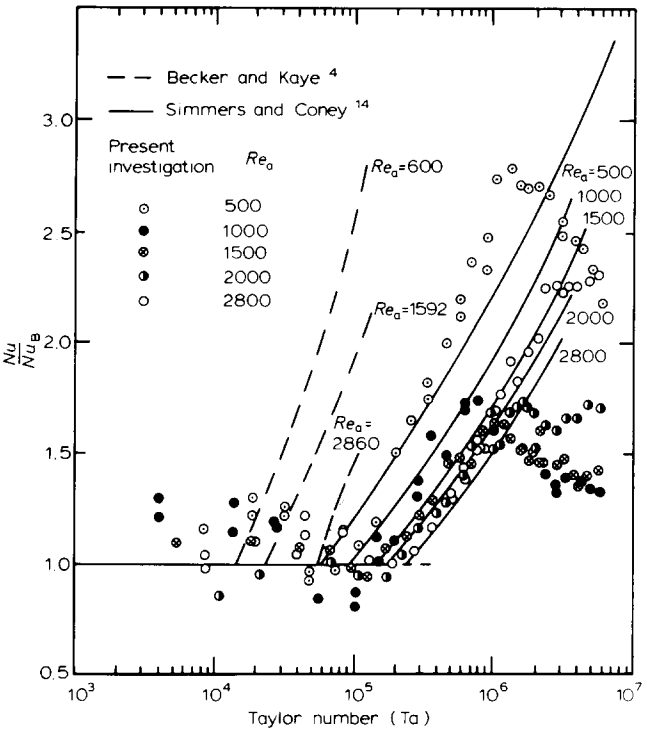

Fig 7 Comparison of wide gap heat transfer data

study. Becker and Kaye[4] considered the inner wall condition for $N = 0.81$ and for a variety of axial flows; their results are compared with the present wide gap results in Fig 7. It can be seen that the earlier results indicate that vortex flow occurs at a lower Taylor number when the inner wall is heated. Of greater interest is the comparison of the present results with the Reynolds analogy solution of Simmers and Coney[14], there being good correspondence up to the point where the third flow regime, occurring at $Ta \approx 10^6$, commences. Because of the limitations of the apparatus, in their experiments, the authors of reference 14 were unable to obtain Taylor numbers much in excess of 10^6 and so did not detect the third flow regime.

Kosterin and Finatev[17], working in the range $3000 \leq Re_a \leq 3 \times 10^4$, found only a continuous increase in Nu with increasing Ta. The heat transfer experiments of Zmeikov and Ustimenko[18] with inner cylinder rotation at turbulent axial Reynolds numbers ($Re_a > 34\,000$), showed similar trends. It is possible that the presence of the third flow regime was not detected because, at higher axial flows, its influence could be reduced. From the evidence so far, this regime of flow seems to have evaded detection by other investigators.

A study of the various modes of diabatic spiral vortex transitions under the influence of high axial velocities has not previously been made. Other investigations[9,11] were confined to the observations of the initial instability with zero or a low axial flow. Snyder[10], working with a heated inner rotating cylinder, noted the growing dependence of his diabatic stability curves on the shape of the imposed axial velocity profile, as the inflection point was displaced by higher axial flows. The conditions of diabatic upflow and downflow were studied by Sorour and

Coney[12] for $Re_a < 1400$. They found that for an imposed axial flow, the point of neutral stability was modified only when natural convection was strong enough to affect the parabolic velocity profile corresponding to that flow, the extent of this modification being dependent on the axial flow direction. They also noticed that the mode of development and the width of the spiral cells were unaffected by the radial thermal gradient. These results are in good agreement with the present investigation for $Re_a = 500$, where values of the critical Taylor number, for both diabatic and adiabatic conditions, were shown to be very similar. No literature is available, however, on the effects of a thermal gradient on the higher transition modes, where the present investigation has shown that a general destabilisation of the flow occurs.

Simmers and Coney[19] measured the diabatic axial, tangential and radial velocity profiles in the wide gap for $Re_a = 400$ and 1200. Their results showed that for Ta in excess of 10^6, the axial profiles flattened over $R' = 0.2$ to $R' = 0.9$, while the tangential velocity profiles exhibited a central region of small velocity gradient bounded by high velocity gradients at the boundaries. From their results, they postulated a mechanism of momentum transfer in the tangential direction whereby 'the vortices rotate as solid bodies, but the outer edges of the vortices actually move through, rather than with, the fluid.' It is possible that the turbulent vortices observed then[19] and in the present study could co-exist with the Görtler form of instability at the outer wall as a result of the steep axial and tangential gradients experienced in that region. Since the velocity components increase as the distance from the centre of curvature of the outer wall decreases, it is probable that, with high velocity gradients, the flow at the outer concave wall will be centrifugally unstable. The rms measurements of Zmeikov and Ustimenko[18] in turbulent axial flow showed that a highly unstable region existed at $R' = 0.9$ with a constant rms value across the gap.

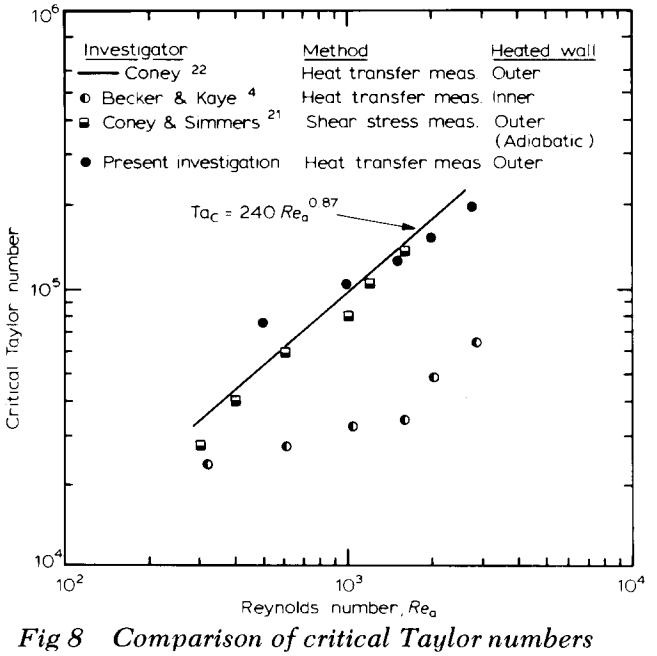

Fig 8 Comparison of critical Taylor numbers

The transfer of energy in the flow preceding the formation of turbulent vortices from a complex flow pattern could be related to the recent work of Mobbs *et al*[20], their digital analysis being performed for zero axial flow in adiabatic conditions. The spectra obtained were converted into wave number spectra using the wave speed. With increase in Ta, the flow became chaotic and rapid wave number changes occurred with greater rates of energy transfer. At very high speeds, the change to a single predominant wave number occurred, having a tendency to a more ordered flow. It is suggested that such an effect may occur in the present investigation. With a heated outer wall, an additional energy source is provided, leading to an earlier onset of this instability.

Diabatic Ta_c for combined axial and rotational flow

Figs 1 and 2 indicate that the onset of vortex flow under diabatic conditions occurs at higher values of Ta than under adiabatic. Also, criticality was not defined, in this study, as the first detectable instability irrespective of its position in the gap, but by the close approach of the vortices to the outer wall, where the thermal boundary layer is reduced by vortex mixing, thereby increasing the heat transfer rates.

Considering the results of Becker and Kaye[4], where the thermal boundary layer is formed near the inner rotating cylinder, which is also the region of maximum instability, it is not surprising that their values of Ta_c correspond closely to those obtained for initial vortex formation.

The values of Ta_c obtained under diabatic conditions by several workers have been compared in Fig 8. The shear stress results of Coney and Simmers[21] were made at the outer wall under adiabatic conditions.

Coney[22] used air as the working fluid and a steam heated outer wall in an apparatus on $N = 0.896$, obtaining the following correlation by means of heat transfer measurements:

$$Ta_c = 240\,Re_a^{0.87} \tag{5}$$

This relationship is shown as a solid line in Fig 8. The Ta_c values resulting from the shear stress measurements[21] and the present data points are seen to lie close to Eq (5). In view of this evidence, it is suggested that a distinct difference occurs between the heated inner wall and the heated outer wall condition for a wide gap. In both cases, an associated thermal boundary layer is formed. For the heated inner wall, the earlier occurrence of vortex flow enhances the rate of heat transfer at that wall, whereas for the heated outer wall, the influence of the vortices on the thermal boundary layers occurs much later and a slightly lower rate of heat transfer is obtained. Hence, with reference to rotary heat exchangers, there is evidence to suggest that a better performance would be obtained with the rotating inner wall as the heat transfer boundary. On the other hand, the complexities associated with having a heated fluid flowing through a rotating tube would be considerable.

Conclusions

It has been shown that the presence of combined axial and rotational vortex flow in an annular gap tends to reduce high temperature gradients in the central region and the vortices are shown to be a highly efficient flow mixing mechanism. From the heat transfer data, three regimes of flow have been found to exist for the range $500 \leq Re_a \leq 2800$ and $3 \times 10^3 \leq Ta \leq 8 \times 10^6$:

- A laminar flow regime over the range of Reynolds number and Taylor number giving an almost uniform Nusselt number.
- A transition to vortex flow (in this case, to the outer wall) forming the secondary regime and giving a sharp increase in Nusselt number.
- A third regime occurring at values of Ta in excess of 10^6 where a reduction in the Nusselt number was observed. This regime has not been detected previously by other workers, owing to the limitations of their Ta values.

The validity of the Reynolds analogy solution of Simmers and Coney[21] has been confirmed within the limits of second flow regimes, good agreement being obtained for the range $1000 \leq Re_a \leq 2800$.

The transition modes of spiral vortex flow, for the range of flows investigated, showed for low values of Re_a the initial vortex instability was independent of the thermal gradient but dependent on the axial velocity. However, a general destabilisation of the higher modes of transition was observed, this being attributed to the increased fluctuations of the mean flow due to the thermal field. For the range $1500 < Re_a < 2500$, a general breakdown of the flow was observed, the damping effects of the axial flow gradually diminishing. Also flow stability in the wide gap occurred over a wider Re_a range than for the narrow gap.

Turbulent vortex formation was found to affect the heat transfer characteristics at the outer wall; the third regime, mentioned above, may be attributed to this flow transition. The mechanism of energy transfer was found to play an important role in turbulent vortex formation and the completion of this transition was followed by a less intense and more ordered flow across the gap. The turbulent vortices were found to have greatest intensity near the outer wall, contrary to the initial spiral vortex instability which occurs near the inner cylinder. The thermal gradient is observed to be conducive to the formation of this transition and the influence of higher axial flows is to delay it.

The heat transfer data provides a good basis for the design of rotary heat exchangers operating within the present experimental range, the heated outer wall condition tending to give slightly lower heat transfer rates compared with a heated wall.

References

1. **Strong A. B. and Carlucci L.** An experimental study of mass transfer in rotating Couette flow with low axial Reynolds numbers. *Canadian J. of Chem. Eng., 1976,* **54**, *295–298*
2. **Luke G. E.** Cooling of electrical machines. *Trans. A.I.E.E., 1923,* **42**, *636–652*
3. **Gazley C.** Heat transfer characteristics of the rotational and axial flow between concentric cylinders. *Trans. A.S.M.E., 1958,* **80**, *79–90*
4. **Becker K. M. and Kaye J.** Measurements of diabatic flow in an annulus with an inner rotating cylinder. *Trans. A.S.M.E., J. Heat Transfer, 1962,* **84**, *97–105*
5. **Fung Y. T. and Kurzweg U. M.** Stability of swirling flows with radius dependent density. *J. Fluid Mech., 1975,* **72**, *Part 2, 243–255*
6. **Withjack E. M. and Chen C. F.** An experimental study of Couette instability of stratified fluids. *J. Fluid Mech., 1974,* **66**, *Part 4, 725–737*
7. **Walowit J., Tsao S. and DiPrima R. C.** Stability of flow between arbitrarily spaced concentric cylindrical surfaces, including the effect of a radial temperature gradient. *Trans. A.S.M.E., J. of Applied Mechanics, 1964, 585–593*
8. **Becker K. M. and Kaye J.** The influence of a radial temperature gradient on the instability of fluid flow in an annulus with an inner rotating cylinder. *Trans. A.S.M.E., J. Heat Transfer, 1962,* **84**, *106–110*
9. **Snyder H. A. and Karlsson S. K. F.** Experiments on the stability of Couette motion with a radial thermal gradient *Phys. Fluids, 1964,* **7**, *No. 10, 1696–1706*
10. **Snyder H. A.** Experiments on the stability of two types of spiral flow. *Annals of Physics, 1965,* **31**, *No. 2, Part 1, 292–313*
11. **Karlsson S. K. F. and Snyder H. A.** Observations on a thermally induced instability between rotating cylinders. *Ann. Phys., 1965,* **31**, *314–324*
12. **Sorour M. M. and Coney J. E. R.** The effect of temperature gradient on the stability of flow between vertical, concentric, rotating cylinders. *J. Mech. Eng. Sci., 1979,* **21**, *No. 6, 403–409*
13. **Wan C. C. and Coney J. E. R.** Transition modes in adiabatic spiral vortex flow in narrow and wide annular gaps. *Int. J. Heat and Fluid Flow, 1980,* **2**, *No. 3, 131–138*
14. **Simmers D. A. and Coney J. E. R.** A Reynolds analogy solution for the heat transfer characteristics of combined Taylor vortex and axial flow. *Int. J. Heat & Mass Transfer, 1979,* **22**, *679–689*
15. **Otnes R. K. and Enochson L.** Digital time series analysis. *John Wiley and Sons, New York, 1972*
16. **Kuzay T. M. and Scott C. J.** Turbulent heat transfer studies in annulus with inner cylinder rotation. *Trans. A.S.M.E., J. Heat Transfer, 1977, 12–19*
17. **Kosterin S. I. and Finatev Y. P.** Heat transfer in turbulent airflow in the annular space between rotating coaxial cylinders. *Inzh. Fiz. Zh.,* **8**, *1962, 3–9*
18. **Zmeikov V. N. and Ustimenko B. P.** Heat and mass transfer: Convective heat exchange in a homogeneous medium, Vol. I. eds *Petukhov B. S., Ginzburg I. P. and Kasperovich A. S., 1965, Nauka i Tekhnika, Minsk*
19. **Simmers D. A. and Coney J. E. R.** Velocity distributions in Taylor vortex flow with imposed axial flow and isothermal surface heat transfer. *Int. J. Heat and Fluid Flow, 1980,* **2**, *No. 2, 85–91*
20. **Mobbs F. R., Preston S. and Ozogan M. S.** An experimental investigation of Taylor vortex waves. *Taylor Vortex Flow Working Party Meeting, Mech. Eng. Dept., University of Leeds, 1979, 53–57*
21. **Coney J. E. R. and Simmers D. A.** The determination of shear stress in fully developed laminar axial flow and Taylor vortex flow, using a flush-mounted hot film probe. *DISA Information, 1979, No. 24, 9–14*
22. **Coney J. E. R.** Taylor vortex flow with special reference to rotary heat exchangers. *Ph.D. thesis, Leeds University, 1971*